

---

# Appendix for Rethinking the Role of Hyperparameter Tuning in Optimizer Benchmarking

---

Yuanhao Xiong<sup>1</sup>, Xuanqing Liu<sup>1</sup>, Li-Cheng Lan<sup>1</sup>, Yang You<sup>2</sup>, Si Si<sup>3</sup>, Cho-Jui Hsieh<sup>1</sup>

<sup>1</sup>Department of Computer Science, UCLA

<sup>2</sup>Department of Computer Science, National University of Singapore

<sup>3</sup>Google Research

{yhxiong,xqliu,lclan}@cs.ucla.edu, youyou@comp.nus.edu.sg  
sisidaisy@google.com, chohsieh@cs.ucla.edu

## 1 A HyperBand

2 We present the whole algorithm for Hyperband in Algorithm 1, and you can refer to Li et al. [7] for  
3 more details.

## 4 B Optimizers

5 **Notations.** Given a vector of parameters  $\theta \in \mathbb{R}^d$ , we denote a sub-vector of its  $i$ -th layer's parameters  
6 by  $\theta^{(i)}$ .  $\{\alpha_t\}_{t=1}^T$  is a sequence of learning rates during the optimization procedure of a horizon  
7  $T$ .  $\{\phi_t, \psi_t\}_{t=1}^T$  represents a sequence of functions to calculate the first-order and second-order  
8 momentum of the gradient  $g_t$ , which are  $m_t$  and  $v_t$  respectively at time step  $t$ . Different optimization  
9 algorithms are usually specified by the choice of  $\phi(\cdot)$  and  $\psi(\cdot)$ .  $\{r_t\}_{t=1}^T$  is an additional sequence of  
10 adaptive terms to modify the magnitude of the learning rate in some methods. For algorithms only  
11 using the first-order momentum,  $\mu$  is the , while  $\beta_1$  and  $\beta_2$  are coefficients to compute the running  
12 averages  $m$  and  $v$ .  $\epsilon$  is a small scalar (e.g.,  $1 \times 10^{-8}$ ) used to prevent division by 0.

13 **Generic optimization framework.** Based on, we further develop a thorough generic optimization  
14 framework including an extra adaptive term in Algorithm 2. The debiasing term used in the original  
15 version of Adam is ignored for simplicity. Note that for  $\{\alpha_t\}_{t=1}^T$ , different learning rate scheduling  
16 strategies can be adopted and the choice of scheduler is also regarded as a tunable hyperparameter.  
17 Without loss of generality, in this paper, we only consider a constant value and a linear decay [10] in  
18 the following equation, introducing  $\gamma$  as a hyperparameter.

$$\alpha_t = \begin{cases} \alpha_0, & \text{constant;} \\ \alpha_0 - (1 - \gamma)\alpha_0 \frac{t}{T}, & \text{linear decay.} \end{cases}$$

19 With this generic framework, we can summarize several popular optimization methods by explicitly  
20 specifying  $m_t$ ,  $v_t$  and  $r_t$  in Table 1. It should be clarified that Lookahead is an exception of the  
21 generic framework. In fact it is more like a high-level mechanism, which can be incorporated with any  
22 other optimizer. However, as stated in Zhang et al. [11], this optimizer is robust to inner optimization  
23 algorithm,  $k$ , and  $\alpha_s$  in Algorithm 3, we still include Lookahead here with Adam as the base for  
24 a more convincing and comprehensive evaluation. We consider Lookahead as a special adaptive  
25 method, and tune the same hyperparameters for it as other adaptive optimizers.

## 26 C Task description

27 We make a concrete description of tasks selected for our optimizer evaluation protocol:

---

**Algorithm 1** Hyperband

---

**Input:**  $R, \eta$ **Initialization:**  $s_{\max} = \lfloor \log_{\eta} R \rfloor, B = (s_{\max} + 1)R$ 

```
1: for  $s \in \{s_{\max}, s_{\max} - 1, \dots, 0\}$  do
2:    $n = \lceil \frac{B}{R} \frac{\eta^s}{(s+1)} \rceil, r = R\eta^{-s}$ 
3:   // begin SuccessiveHalving with  $(n, r)$  inner loop
4:    $T = \text{random\_get\_configuration}(n)$ 
5:   for  $i \in \{0, \dots, s\}$  do
6:      $n_i = \lfloor n\eta^{-i} \rfloor, r_i = r\eta^i$ 
7:      $L = \{\text{run\_then\_return\_val\_loss}(t, r_i) : t \in T\}$ 
8:      $T = \text{top\_k}(T, L, \lfloor n_i/\eta \rfloor)$ 
9:   end for
10: end for
Return Hyperparameter configuration with the smallest loss seen so far
```

---

---

**Algorithm 2** Generic framework of optimization methods

---

**Input:** parameter value  $\theta_1$ , learning rate with scheduling  $\{\alpha_t\}$ , sequence of functions  $\{\phi_t, \psi_t, \chi_t\}_{t=1}^T$  to compute  $m_t, v_t$ , and  $r_t$  respectively.

```
1: for  $t = 1$  to  $T$  do
2:    $g_t = \nabla f_t(\theta_t)$ 
3:    $m_t = \phi_t(g_1, \dots, g_t)$ 
4:    $v_t = \psi_t(g_1, \dots, g_t)$ 
5:    $r_t = \chi_t(\theta_t, m_t, v_t)$ 
6:    $\theta_{t+1} = \theta_t - \alpha_t r_t m_t / \sqrt{v_t}$ 
7: end for
```

---

- 28 • Image classification. For this task, we adopt a ResNet-50 [5] model on CIFAR10 and CIFAR100  
29 with a batch size of 128 and the maximum epoch of 200 per trial.
- 30 • VAE. We use a vanilla variational autoencoder in Kingma and Welling [6] with five convolutional  
31 and five deconvolutional layers with a latent space of dimension 128 on CelebA. There are no  
32 dropout layers. Trained with a batch size of 144.
- 33 • GAN. We train SNGAN with the same network architecture and objective function with spectral  
34 normalization for CIFAR10 in Miyato et al. [8], and the batch size of the generator and the  
35 discriminator is 128 and 64 respectively.
- 36 • Natural language processing. In this domain, we finetune RoBERTa-base on MRPC, one of the test  
37 suit in GLUE benchmark. For each optimizer, we set the maximal exploration budget to be 800  
38 epochs. The batch size is 16 sentences.
- 39 • Graph learning. Among various graph learning problems, we choose node classification as semi-  
40 supervised classification. In GCN training, in there are multiple ways to deal with the neighborhood  
41 explosion of stochastic optimizers. We choose Cluster-GCN [4] as the backbone to handle neigh-  
42 borhood expansion and PPI as the dataset.
- 43 • Reinforcement learning. We select Walker2d-v3 from OpenAI Gym ([3]) as our training environ-  
44 ment, and PPO ([9]), implemented by OpenAI SpinningUp ([1]), as the algorithm that required  
45 tuning. We use the same architectures for both action value network  $Q$  and the policy network  $\pi$ .  
46 We define 40,000 of environment interactions as one epoch, with a batch size of 4,000. The return  
47 we used is the highest average test return of an epoch during the training.

## 48 D Implementation Details

49 Implementation details of our experiments are provided in this section. Specifically, we give the  
50 unified search space for all hyperparameters and their default values in Table 2. Note that we tune the  
51 learning rate decay factor for image classification tasks when tuning every hyperparameter. For the  
52 task on MRPC,  $\gamma$  is tuned for all experiments. In other cases, we only tune original hyperparameters  
53 without a learning rate scheduler.

Table 1: A summary of popular optimization algorithms with different choices of  $m_t$ ,  $v_t$  and  $r_t$ .

	$m_t$	$v_t$	$r_t$
SGD(M)	$\mu m_{t-1} + g_t$	1	1
Adam	$\beta_1 m_{t-1} + (1 - \beta_1) g_t$	$\beta_2 v_{t-1} + (1 - \beta_2) g_t^2$	1
RADam	$\beta_1 m_{t-1} + (1 - \beta_1) g_t$	$\beta_2 v_{t-1} + (1 - \beta_2) g_t^2$	$\sqrt{\frac{(\rho_t - 4)(\rho_t - 2)\rho_\infty}{(\rho_\infty - 4)(\rho_\infty - 2)\rho_t}}$
Yogi	$\beta_1 m_{t-1} + (1 - \beta_1) g_t$	$v_{t-1} - (1 - \beta_2) \text{sign}(v_{t-1} - g_t^2) g_t^2$	1
LARS	$\mu m_{t-1} + g_t$	1	$\frac{\ \theta_t^{(i)}\ }{\ m_t^{(i)}\ }$
LAMB	$\beta_1 m_{t-1} + (1 - \beta_1) g_t$	$\beta_2 v_{t-1} + (1 - \beta_2) g_t^2$	$\frac{\ \theta_t^{(i)}\ }{\ m_t^{(i)} / \sqrt{v_t^{(i)}}\ }$
Lookahead*	$\beta_1 m_{t-1} + (1 - \beta_1) g_t$	$\beta_2 v_{t-1} + (1 - \beta_2) g_t^2$	1

---

**Algorithm 3** Lookahead Optimizer

---

**Input:** Initial parameters  $\theta_0$ , objective function  $f$ , synchronization period  $k$ , slow weights step size  $\alpha_s$ , optimizer  $A$

```

1: for  $t = 1, 2, \dots$  do
2:   Synchronize parameters  $\hat{\theta}_{t,0} \leftarrow \theta_{t-1}$ 
3:   for  $i = 1, 2, \dots, k$  do
4:     Sample minibatch of data  $d \in \mathcal{D}$ 
5:      $\hat{\theta}_{t,i} \leftarrow \hat{\theta}_{t,i-1} + A(L, \hat{\theta}_{t,i-1}, d)$ 
6:   end for
7:   Perform outer update  $\theta_t \leftarrow \theta_{t-1} + \alpha_s(\hat{\theta}_{t,k} - \theta_{t-1})$ 
8: end for

```

**Return** Parameters  $\theta$

---

54 In addition, Hyperband parameter values for each task are listed in Table 3. These parameters are assigned based on properties of different tasks.

Table 2: Hyperparameter search space and default value

Hyperparameter	Search space	Default value
$\alpha_0$	Log-Uniform( $-8, 1$ )	$\times$
$\mu$	Uniform[ $0, 1$ ]	0 for SGD and 0.9 for LARS
$1 - \beta_1$	Log-Uniform( $-4, 0$ )	0.1
$1 - \beta_2$	Log-Uniform( $-6, 0$ )	0.001
$\epsilon$	Log-Uniform( $-8, 1$ )	1e-8
$\gamma$	Log-Uniform( $-4, 0$ )	$\times$

55

56 For time cost of our evaluation protocols, it depends on how many budgets are available. Specifically,  
57 in our paper, the unit of time budget is one epoch, then the total time will be  $B_{epoch} * T_{epoch}$ , where  
58  $B_{epoch}$  is the total available budget and  $T_{epoch}$  is the running time for one epoch. There is no  
59 additional computational cost, i.e., running our protocol once takes the same time as running one  
60 hyperparameter search with Hyperband. In our experiment on CIFAR10, we roughly evaluated 200  
61 hyperparameter configurations in one Hyperband running, while the same time can only allow about  
62 50 configurations in random search.

63 Moreover, we can further accelerate our evaluation protocol by resampling, shown in Algorithm  
64 4. The basic idea is that we keep a library of different hyperparameter settings. At the beginning,  
65 the library is empty. And in each repetition, we sample a number of configurations required by  
66 running Hyperband once. During the simulation of Hyperband, we just retrieve the value from the  
67 library if the desired epoch of current configuration is contained in the library. Otherwise, we run this  
68 configuration based on Hyperband, and store the piece of the trajectory to the library.

69 **E Additional results**

70 More detailed experimental results are reported in this section.

Table 3: Hyperband parameters for each task.

Task	Hyperband parameter		
	$R$	$n_c$	$\eta$
Image Classification	200	172	$\eta = 3$
VAE	50	62	
GAN	200	172	
GLUE benchmark	10	200	
Graph learning	200	200	
RL	200	172	

**Algorithm 4** Alternative End-to-End Efficiency Evaluation Protocol

**Input:** A set of optimizers  $\mathcal{O} = \{o : o = (\mathcal{U}, \Omega)\}$ , task  $a \in \mathcal{A}$ , search space  $\mathcal{F}$ , library size  $S$

- 1: **for**  $o \in \mathcal{O}$  **do**
- 2:   Sample  $S$  configurations from  $\mathcal{F}$ , initialize the library with an empty list for each setting
- 3:   **for**  $i = 1$  **to**  $M$  **do**
- 4:     Simulate Hyperband with  $o$  using configurations re-sampled from the library on  $a$
- 5:     **if** the desired accuracy is pre-computed in the library **then**
- 6:       Retrieve the value directly
- 7:     **else**
- 8:       Training normally, and store values to the library
- 9:     **end if**
- 10:    Record the performance trajectory  $\{P_t\}_{t=1}^T$  explored by HyperBand
- 11:    Calculate the peak performance and  $CPE$  by Eq. 1
- 12:    **end for**
- 13:    Average peak and  $CPE$  values over  $M$  repetitions for the optimizer  $o$
- 14: **end for**
- 15: Evaluate optimizers according to their peak and  $CPE$  values

71 **E.1 Impact of  $\eta$** 

72 Since there is an extra hyperparameter, the reduction factor  $\eta$  in Hyperband, we conduct an experiment  
 73 with different values ( $\eta = 2, 3, 4, 5$ ) to observe the potential impact of this additional hyperparameter  
 74 on our evaluation. Specifically, we use Hyperband to tune the learning rate for three optimizers, SGD,  
 75 Adam, and Lookahead on CIFAR10, and results are presented in Table 4. As we can see, although  
 76 the change of  $\eta$  may lead to different CPE values, the relative ranking among three optimizers  
 77 remains unchanged. Besides, they all achieve comparable peak performance at the end of training.  
 78 Considering the efficiency of Hyperband, we choose  $\eta = 3$  based on the convention in Li et al. [7] in  
 79 all our experiments.

Table 4: CPE on CIFAR10 with different  $\eta$ . The value in the round brackets is peak performance.

Optimizer	CIFAR10 (%) $\uparrow$			
	$\eta = 2$	$\eta = 3$	$\eta = 4$	$\eta = 5$
<i>Tune learning rate only:</i>				
SGD	88.63 (93.42)	88.87 (93.39)	88.45 (93.34)	87.97(93.73)
Adam	90.35 (93.24)	90.42 (93.65)	90.06 (93.26)	88.75 (93.23)
Lookahead	90.46 (93.53)	90.60 (93.60)	90.33 (93.40)	89.05 (93.62)

80 **E.2 End-to-end training**

81 Table 5 shows peak performance for optimizers on each task. For GAN, we only conduct evaluation  
 82 on optimizers tuning learning rate due to time limit, and present its CPE and peak performance in  
 83 Table 6. There is also an end-to-end training curve for GAN on CIFAR10 in Figure 1. Figures for  
 84 end-to-end training curves on the rest of tasks are shown in Figure 4 and 5.

Table 5: Peak performance during end-to-end training. The best one for each task is highlighted in bold.

Optimizer	CIFAR10 (%) $\uparrow$ (classification)	CIFAR100 (%) $\uparrow$ (classification)	CelebA $\downarrow$ (VAE)	MRPC (%) $\uparrow$ (NLP)	PPI $\uparrow$ (GCN)	Walker2d-v3 $\uparrow$ (RL)
<i>Tune learning rate only:</i>						
SGD	93.39 $\pm$ 0.12	<b>73.68 <math>\pm</math> 0.13</b>	0.1351 $\pm$ 0.0003	71.05 $\pm$ 0.25	94.74 $\pm$ 2.7 $\times 10^{-2}$	3589 $\pm$ 221
Adam	93.65 $\pm$ 0.13	71.51 $\pm$ 0.21	0.1326 $\pm$ 0.0001	84.90 $\pm$ 0.10	<b>98.73 <math>\pm</math> 5.9 <math>\times 10^{-4}</math></b>	4735 $\pm$ 91
RAdam	<b>93.93 <math>\pm</math> 0.09</b>	72.30 $\pm$ 0.09	<b>0.1325 <math>\pm</math> 0.0002</b>	<b>85.41 <math>\pm</math> 1.45</b>	98.70 $\pm$ 1.0 $\times 10^{-3}$	5020 $\pm$ 112
Yogi	93.58 $\pm$ 0.03	73.48 $\pm$ 0.93	0.1334 $\pm$ 0.0002	70.19 $\pm$ 0.92	98.18 $\pm$ 9.0 $\times 10^{-4}$	5013 $\pm$ 439
LARS	93.46 $\pm$ 0.01	73.53 $\pm$ 0.17	0.1332 $\pm$ 0.0001	68.97 $\pm$ 0.85	98.45 $\pm$ 4.7 $\times 10^{-4}$	4073 $\pm$ 443
LAMB	93.39 $\pm$ 0.03	70.38 $\pm$ 0.08	0.1329 $\pm$ 0.0002	82.23 $\pm$ 0.78	98.46 $\pm$ 2.2 $\times 10^{-4}$	4219 $\pm$ 191
Lookahead	93.60 $\pm$ 0.04	71.75 $\pm$ 0.68	0.1327 $\pm$ 0.0001	72.99 $\pm$ 0.61	98.63 $\pm$ 1.4 $\times 10^{-3}$	<b>5246 <math>\pm</math> 666</b>
<i>Tune every hyperparameter:</i>						
SGD	93.47 $\pm$ 0.02	<b>73.94 <math>\pm</math> 0.06</b>	0.1344 $\pm$ 0.0003	72.80 $\pm$ 1.58	98.64 $\pm$ 1.5 $\times 10^{-3}$	3647 $\pm$ 129
Adam	92.58 $\pm$ 1.63	73.82 $\pm$ 0.25	0.1327 $\pm$ 0.0002	88.46 $\pm$ 0.66	<b>98.93 <math>\pm</math> 7.5 <math>\times 10^{-4}</math></b>	<b>4986 <math>\pm</math> 404</b>
RAdam	<b>94.47 <math>\pm</math> 0.24</b>	73.50 $\pm$ 0.32	<b>0.1326 <math>\pm</math> 0.0001</b>	<b>88.78 <math>\pm</math> 0.72</b>	98.92 $\pm$ 6.0 $\times 10^{-4}$	4886 $\pm$ 334
Yogi	93.75 $\pm$ 0.08	73.88 $\pm$ 0.25	0.1333 $\pm$ 0.0004	69.60 $\pm$ 1.20	98.85 $\pm$ 4.8 $\times 10^{-4}$	4612 $\pm$ 370
LARS	94.22 $\pm$ 0.10	74.08 $\pm$ 0.04	0.1333 $\pm$ 0.0003	79.83 $\pm$ 6.50	98.88 $\pm$ 8.4 $\times 10^{-4}$	3526 $\pm$ 312
LAMB	93.88 $\pm$ 0.32	71.31 $\pm$ 0.08	0.1332 $\pm$ 0.0002	87.80 $\pm$ 1.07	98.80 $\pm$ 1.0 $\times 10^{-3}$	3654 $\pm$ 243
Lookahead	93.82 $\pm$ 0.18	72.90 $\pm$ 0.85	0.1330 $\pm$ 0.0005	86.15 $\pm$ 0.69	98.87 $\pm$ 1.9 $\times 10^{-3}$	4614 $\pm$ 96

Table 6: CPE on GAN for end-to-end training. The value in the bracket is peak performance.

Optimizer	GAN-CIFAR10 $\downarrow$
<i>Tune learning rate only:</i>	
SGD	113.25 (50.08)
Adam	77.04 (25.14)
RAdam	73.85 (19.61)
Yogi	76.80 (25.36)
LARS	157.71 (73.82)
LAMB	68.47 (25.55)
Lookahead	<b>65.61 (20.40)</b>

85 Besides the general performance profile, we present a probabilistic version described in Barreto et al.  
 86 [2] in Figure 2 to account for randomness. The probabilistic performance profile can be formulated  
 87 as

$$\bar{\rho}_o(\tau) = \frac{1}{|\mathcal{A}|} \sum_a \mathcal{P}(\bar{r}_{o,a} \leq \tau), \quad \bar{r}_{o,a} \sim \mathcal{N}\left(\frac{\mu_{o,a}}{b_a}, \frac{\sigma_{o,a}^2}{b_a^2}\right), \quad (1)$$

88 where  $\mu_{o,a}$  and  $\sigma_{o,a}$  are the mean and standard deviation of CPE of the optimizer  $o$  on the task  $a$   
 89 respectively, and  $b_a$  is just the best expectation of CPE on  $a$  among all optimizers. It can be seen in  
 90 Figure 2 that the probabilistic performance profiles shows a similar trend to Figure 4 in the main  
 91 paper.

92 We also attach two end-to-end training trajectories on CIFAR10 with the error in Figure 3. Since it is  
 93 hard to distinguish optimizers with the standard deviation added, we just instead report the std of  
 94 CPE and peak performance.

### 95 E.3 Data addition training

96 We provide training curves for data-addition training on full MRPC and PPI dataset in Figure 6.

### 97 E.4 Training time comparison

98 In this part, we report training time for each optimizer of running one epoch on CIFAR100 in Table 7.  
 99 As we can see, SGD runs faster than all other advanced optimizers. Besides, we plot the performance  
 100 of different optimizers along with the training time in Figure 7. Here the unit is the running time  
 101 for one epoch of SGD. The relative ranking of selected optimizers is consistent with that under the  
 102 budget of training epochs.

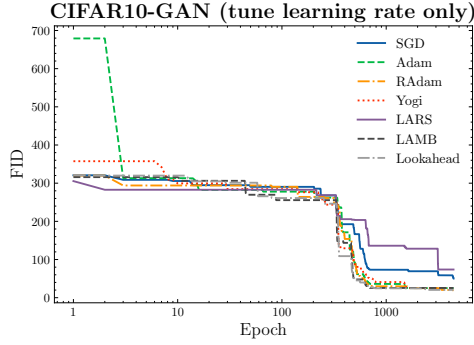
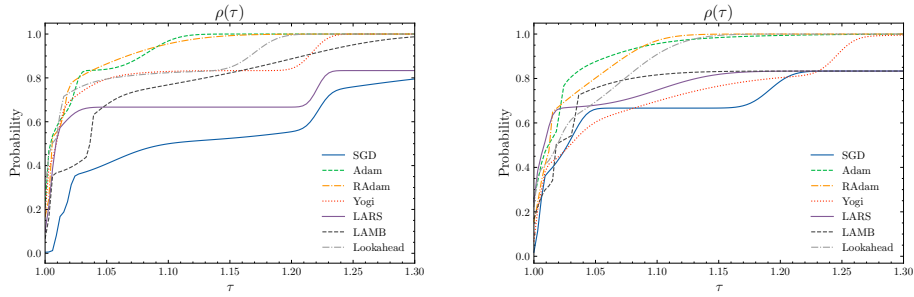


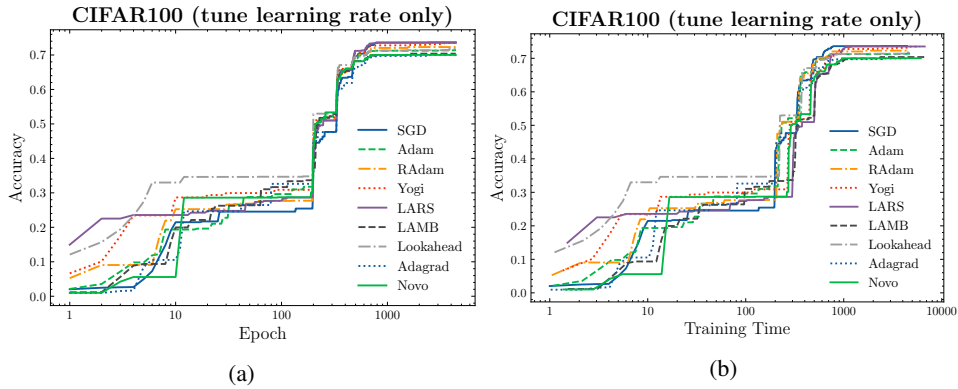
Figure 1: End-to-end training curves for GAN on CIFAR10.



(a) Tune learning rate only.

(b) Tune every hyperparameter.

Figure 2: Probabilistic performance profile of 7 optimizers in the range [1.0, 1.3].



(a)

(b)

Figure 7: End-to-end training curves on CIFAR100 of different time budget units: epoch and training time.

## 103 References

- 104 [1] Joshua Achiam. Spinning Up in Deep Reinforcement Learning, 2018.
- 105 [2] André MS Barreto, Heder S Bernardino, and Helio JC Barbosa. Probabilistic performance  
106 profiles for the experimental evaluation of stochastic algorithms. In *Proceedings of the 12th*  
107 *annual conference on Genetic and evolutionary computation*, pages 751–758, 2010.
- 108 [3] Greg Brockman, Vicki Cheung, Ludwig Pettersson, Jonas Schneider, John Schulman, Jie Tang,  
109 and Wojciech Zaremba. Openai gym, 2016.
- 110 [4] Wei-Lin Chiang, Xuanqing Liu, Si Si, Yang Li, Samy Bengio, and Cho-Jui Hsieh. Cluster-gcn:  
111 An efficient algorithm for training deep and large graph convolutional networks. In *Proceedings*

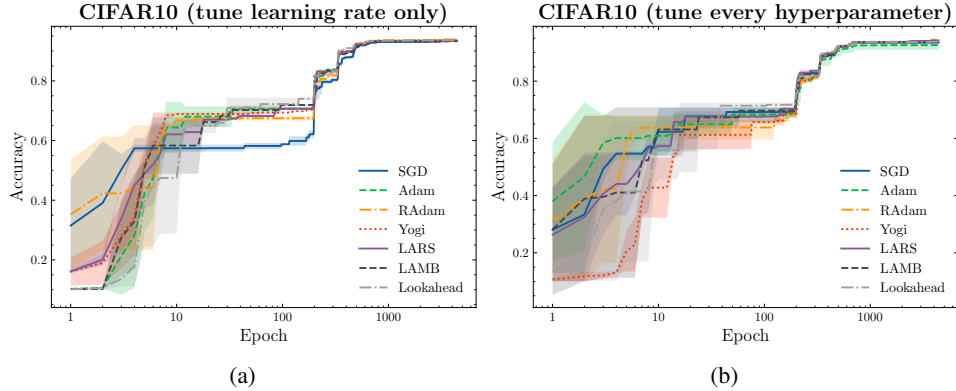


Figure 3: End-to-end training curves on CIFAR10

Table 7: Training time of optimizers for running one epoch on CIFAR100 (unit: second).

Optimizer	SGD	Adam	RAdam	Yogi	LARS	LAMB	Lookahead	Adagrad	NovoGrad
<b>Training Time</b>	<b>43.19</b>	58.43	46.29	66.00	65.47	48.32	45.26	44.18	59.85

112 of the 25th ACM SIGKDD International Conference on Knowledge Discovery & Data Mining,  
 113 pages 257–266, 2019.

114 [5] Kaiming He, Xiangyu Zhang, Shaoqing Ren, and Jian Sun. Deep residual learning for image  
 115 recognition. In *Proceedings of the IEEE conference on computer vision and pattern recognition*,  
 116 pages 770–778, 2016.

117 [6] Diederik P Kingma and Max Welling. Auto-encoding variational bayes. *arXiv preprint*  
 118 *arXiv:1312.6114*, 2013.

119 [7] Lisha Li, Kevin Jamieson, Giulia DeSalvo, Afshin Rostamizadeh, and Ameet Talwalkar. Hyper-  
 120 band: A novel bandit-based approach to hyperparameter optimization. *The Journal of Machine*  
 121 *Learning Research*, 18(1):6765–6816, 2017.

122 [8] Takeru Miyato, Toshiki Kataoka, Masanori Koyama, and Yuichi Yoshida. Spectral normalization  
 123 for generative adversarial networks. *arXiv preprint arXiv:1802.05957*, 2018.

124 [9] John Schulman, Filip Wolski, Prafulla Dhariwal, Alec Radford, and Oleg Klimov. Proximal  
 125 policy optimization algorithms. *arXiv preprint arXiv:1707.06347*, 2017.

126 [10] Christopher J Shallue, Jaehoon Lee, Joseph Antognini, Jascha Sohl-Dickstein, Roy Frostig, and  
 127 George E Dahl. Measuring the effects of data parallelism on neural network training. *arXiv*  
 128 *preprint arXiv:1811.03600*, 2018.

129 [11] Michael Zhang, James Lucas, Jimmy Ba, and Geoffrey E Hinton. Lookahead optimizer: k steps  
 130 forward, 1 step back. In *Advances in Neural Information Processing Systems*, pages 9597–9608,  
 131 2019.

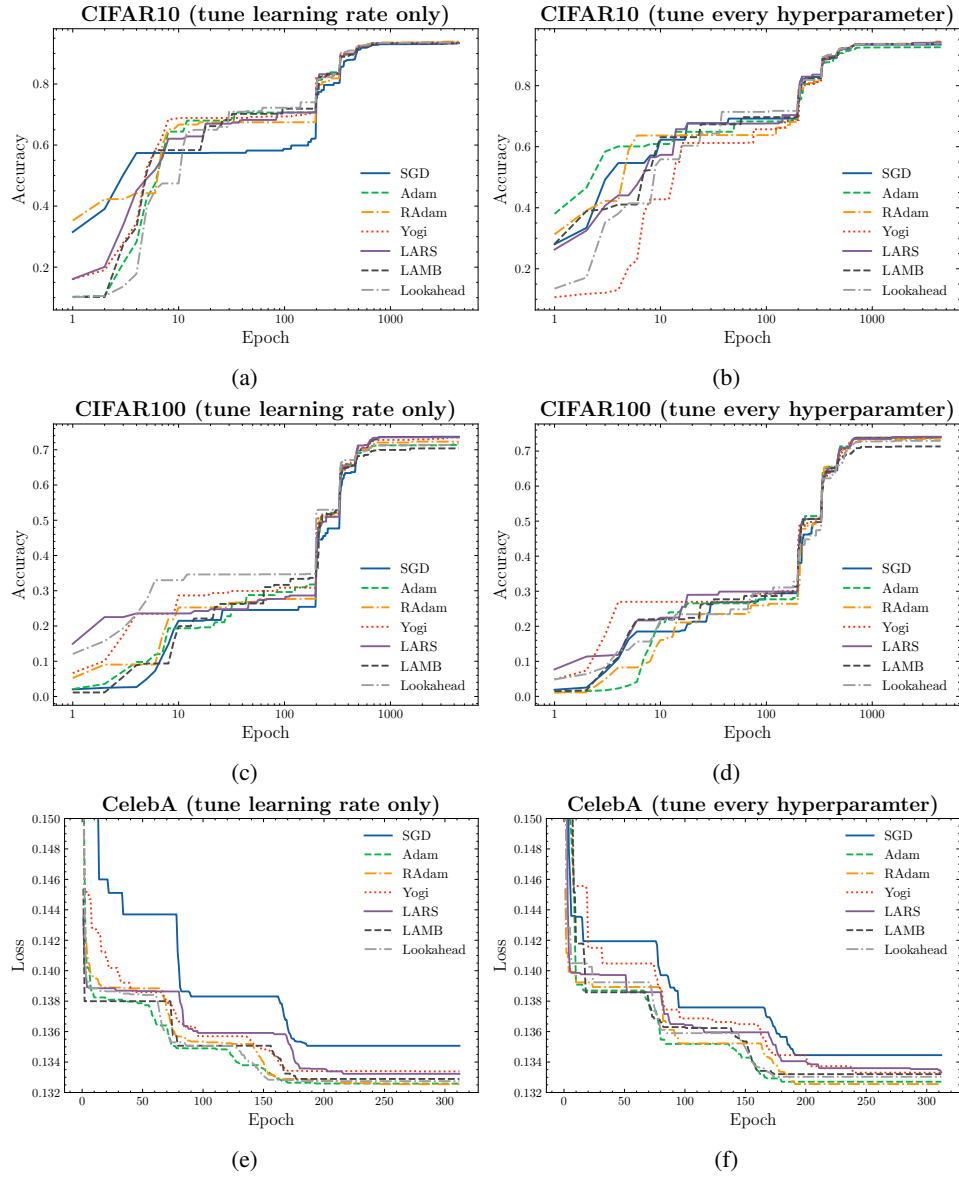


Figure 4: End-to-end training curves on CIFAR10, CIFAR100, and CelebA.

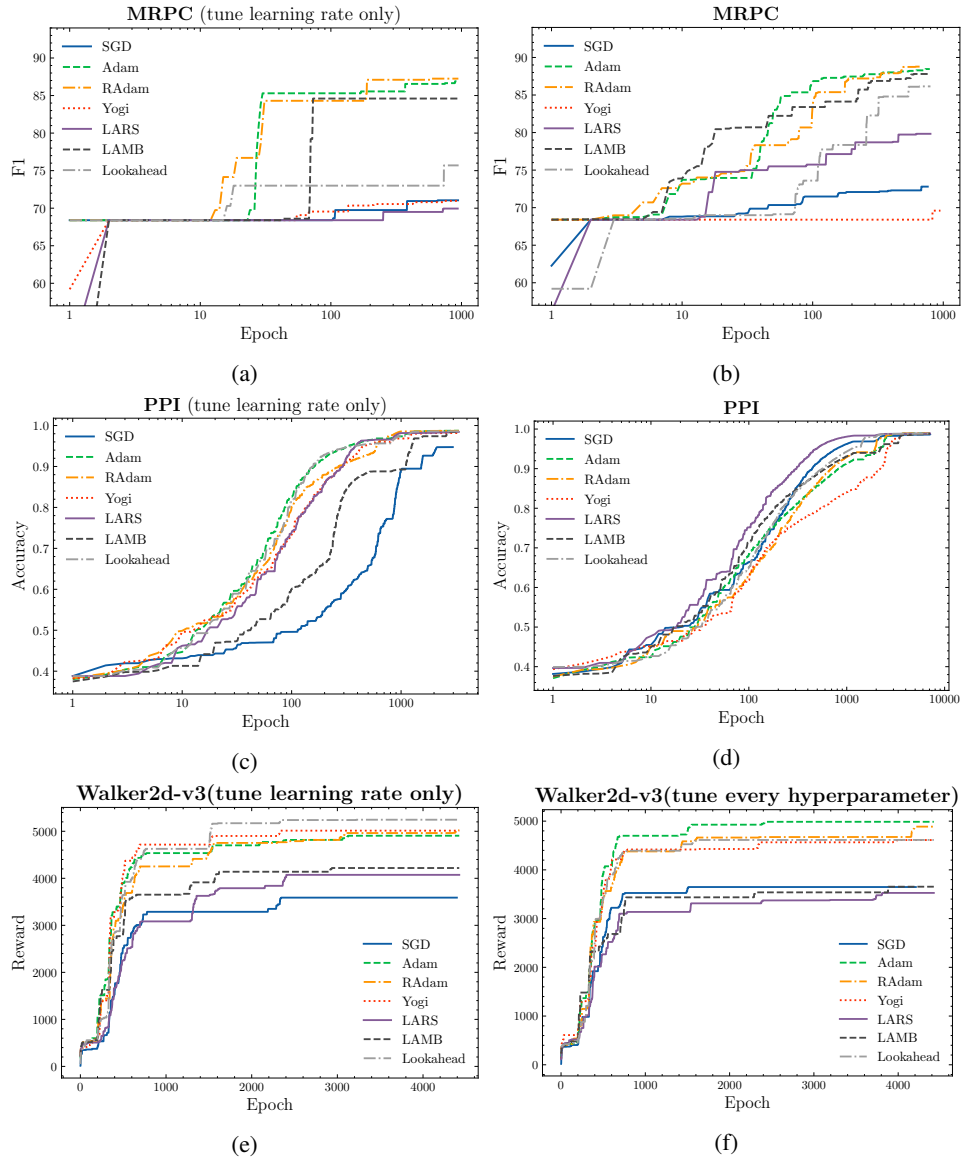
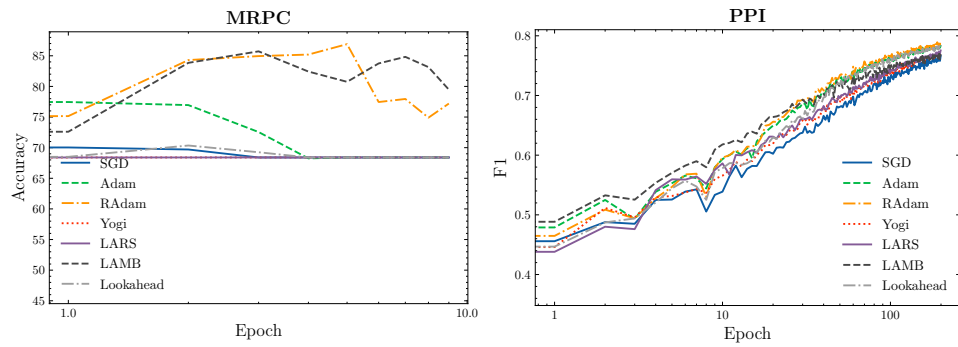


Figure 5: End-to-end training curves on MRPC, PPI, and Walker2d-v3.



(a) Training on full MRPC.

(b) Training on full PPI.

Figure 6: Data addition training on MRPC and PPI.